Experimental Validation of Intent Sharing in Cooperative Maneuvering

Hao M. Wang, Sergei S. Avedisov, Onur Altintas, and Gábor Orosz

2023 IEEE Intelligent Vehicles Symposium (IV) | 979-8-3503-4691-6/23/$31.00 ©2023 IEEE | DOI: 10.1109/IV55152.2023.10186821

***Abstract*— Intent sharing is an emerging type of vehicle-to-everything (V2X) communication where vehicles share information about their intended future trajectories. In this study, we implement intent sharing via commercially available V2X devices, and experimentally demonstrate its benefits in resolving conflicts arising in cooperative maneuvering. An extended framework of conflict analysis is used to provide decision-making assistance via on-board warnings to a human-driven vehicle in highway merge scenario. We show that intent information can significantly benefit safety and time efficiency. Using the experimental data, we also evaluate the effects of communication conditions (e.g., sending rate and intent horizon) on the gained benefits.**

I. Introduction

Emerging technologies in vehicular automation and communication brought new opportunities to enhance traffic safety and efficiency by allowing conflict resolution between vehicles in a cooperative fashion [1]. In a fully automated environment, prior works show that vehicle-to-everything (V2X) communication can enable vehicles to negotiate their future trajectories via maneuver coordination messages [2], [3] while applying a number of control techniques [4], [5].

In the coming decades, mixed-autonomy is expected to be the dominant traffic environment, where vehicles of different automation levels and cooperation classes share the roads [6], [7]. In such a mixed environment, negotiation may not always be feasible, but vehicles may cooperate by sharing their status and intent. Status sharing allows connected vehicles to exchange status information such as position and velocity. The basic safety message (BSM) is a standardized example of status sharing [8]. In intent sharing, the information regarding future motion is shared (e.g., velocity and acceleration bounds over a future time horizon) [7]. Status information makes a vehicle aware of its instantaneous environment, and can lead to inefficient decisions or abrupt actions due to the lack of anticipation on future uncertainty. On the other hand, as an emerging type of cooperation, intent sharing can benefit a vehicle's decision and control by enabling a more accurate prediction of the future environment.

Standardization of intent sharing cooperation is currently in progress [9]–[11], but no actual intent messages have been developed and field-tested so far. Envisioning the future deployment of intent sharing communication, in our previous works [12], [13] we developed a tool called conflict analysis to interpret status and intent information. This tool enables fast and reliable decision-making and controller design to ensure conflict-free maneuvers in mixed traffic. However, previous studies on intent sharing were restricted to theory, and to the best of our knowledge, there is no existing work in the literature experimentally evaluating the benefits of intent sharing using real connected vehicles.

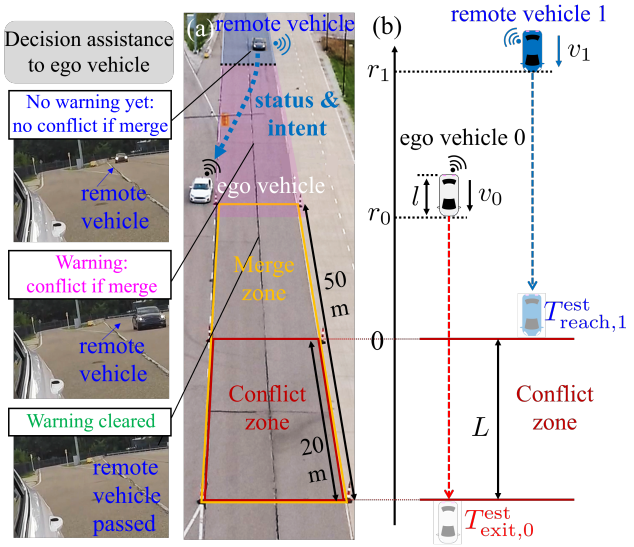

Fig. 1. Experimental setup for validating intent sharing communication in cooperative maneuvering. (a) A merge scenario where intent-based decision assistance is provided to the on-ramp ego vehicle. The leftmost column shows views from the ego vehicle's rear mirror. (b) Generalized model.

In this study, we implement intent sharing using commercially available V2X communication devices, and experimentally validate conflict resolution on a closed test track. In Fig. 1(a), an on-ramp ego vehicle attempts to merge onto the main road while receiving status and intent messages from a vehicle approaching on the main road. We extend the aforementioned conflict analysis framework to help the decision-making of the human-driven ego vehicle to achieve a conflict-free maneuver while taking into account the driver's behavior preferences and uncertainty. We experimentally demonstrate that compared to sharing only status information, intent messages can significantly reduce the inefficiency in decision, contributing to better time efficiency and traffic throughput. A metric is proposed to quantify such benefits, with which we evaluate the effects of intent sharing communication conditions, such as intent horizon and message sending rate, on conflict resolution. Most importantly, we develop and validate an on-board decision assistance system that benefits a human driver's decision-making in real time.

Hao M. Wang and Gábor Orosz are with the Department of Mechanical Engineering, University of Michigan, Ann Arbor, MI 48109, USA. {haowangm, orosz}@umich.edu.

Sergei S. Avedisov and Onur Altintas are with Toyota Motor North America R&D – InfoTech Labs, Mountain View, CA 94043, USA. {sergei.avedisov, onur.altintas}@toyota.com.

Gábor Orosz is also with the Department of Civil and Environmental Engineering, University of Michigan, Ann Arbor, MI 48109, USA.

II. Intent Sharing in Cooperative Maneuvering

In this section, we construct mathematical models of vehicle dynamics. Using these models we formally define vehicle intent. Then we show how to create and transmit intent messages using V2X devices on real vehicles.

A. Modeling vehicle dynamics and communication

We consider the merge scenario depicted in Fig. 1(a) as an application example for intent sharing cooperation. Here, the ego vehicle 0 (white) seeks to merge onto the main road within a merge zone (yellow rectangle) while remote vehicle 1 (blue) is approaching. We define a conflict zone near the end of the merge zone as highlighted by the red rectangle. A conflict happens if both vehicles appear (even partially) in the conflict zone at the same time. A generalized model is shown in Fig. 1(b) focusing on the longitudinal dynamics of the vehicles. Here, r_0 and r_1 denote the positions of the vehicles' front bumpers, while v_0 and v_1 denote their longitudinal velocities. We use L to denote the length of conflict zone whose start position is set to be the origin. Without loss of generality, both vehicles are considered to have the same length ℓ, and we define $s := L + \ell$.

The vehicles' longitudinal dynamics are given such that we neglect air drag and rolling resistance for simplicity:

$$\dot{r}_i(t) = -v_i(t), \qquad \dot{v}_i(t) = \mathrm{sat}(u_i(t)), \qquad i = 0, 1. \tag{1}$$

Here the dot represents time derivative, and u_i are the control inputs (acceleration) of both vehicles. The negative sign in front of the velocity indicates that the vehicles are traveling towards the negative direction in our coordinate system. We use the saturation function $\mathrm{sat}(\cdot)$ to model the acceleration limits, where for $v \in (v_{\min}, v_{\max})$ we have

$$\mathrm{sat}(u) = \max\big\{\min\{u, a_{\max}\}, a_{\min}\big\}. \tag{2}$$

For $v = v_{\max}$, we replace $a_{\max}$ with zero since further accelerating is not allowed; for $v = v_{\min}$, we replace $a_{\min}$ with zero since further decelerating is not allowed. Table I summarizes the values of these limits corresponding to our experimental setup as discussed further below. The system state is defined as

$$\mathbf{x} := \begin{bmatrix} r_0 & v_0 & r_1 & v_1 \end{bmatrix}^\top \in \Omega, \tag{3}$$

where the state space Ω is given by

$$\Omega := [-s, \infty) \times [v_{\min,0}, v_{\max,0}] \times [-s, \infty) \times [v_{\min,1}, v_{\max,1}]. \tag{4}$$

Note that here, the remote vehicle 1 is assumed to be out of our control. That is, we cannot prescribe input u_1 nor do we have the knowledge about the exact value of u_1 (except for its limits).

TABLE I

Parameter values used in the paper.

L	20 [m]	l	5 [m]
$a_{\min,0}$	-4 [m/s^2]	$a_{\min,1}$	-4 [m/s^2]
$a_{\max,0}$	4 [m/s^2]	$a_{\max,1}$	4 [m/s^2]
$v_{\min,0}$	0 [m/s]	$v_{\min,1}$	8 [m/s]
$v_{\max,0}$	15 [m/s]	$v_{\max,1}$	15 [m/s]

Utilizing two classes of V2X communication: status sharing and intent sharing, we aim to help a human-driven ego vehicle to prevent conflict with the approaching. In particular, we assist the driver's decision-making whether to merge ahead of the approaching vehicle or not. The details of decision-making assistance is discussed in Section III, while here we present details of communication setup. In status sharing, the ego vehicle periodically obtains the most recent motion information from the remote vehicle, i.e., r_1 and v_1. In intent sharing information regarding the remote vehicle's future behavior is available. For the merge scenario, a formal definition of the remote vehicle's longitudinal motion intent is given below.

Definition 1: Given the dynamics (1)-(2), the intent of remote vehicle 1's longitudinal motion is represented by a lane number n, a restricted velocity domain $v_1(t) \in [\underline{v}_1, \overline{v}_1]$ and acceleration (input) domain $u_1(t) \in [\underline{a}_1, \overline{a}_1]$ over the time period $t \in [\tilde{t}, \tilde{t} + \Delta t]$. Here $\tilde{t}$ is the time when this intent is generated, Δt is the intent horizon, and $v_{\min,1} \le \underline{v}_1 \le \overline{v}_1 \le v_{\max,1}$, $a_{\min,1} \le \underline{a}_1 \le \overline{a}_1 \le a_{\max,1}$. ■

For example, an intent message may contain the information that for the next $\Delta t = 10$ [s], the remote vehicle 1 will be traveling on the rightmost lane (with lane number $n = 0$) with velocity between $\underline{v}_1 = 13$ and $\overline{v}_1 = 15$ [m/s], and acceleration between $\underline{a}_1 = -0.8$ and $\overline{a}_1 = 1.2$ [m/s^2].

We emphasize that Definition 1 enables a vehicle's intent to be encoded into a set of parameters describing the intended bounds of kinematic/dynamic variables. This compact representation enables a continuous-time prediction of the intent sender's possible future trajectories, which is applicable to most traffic scenarios and maneuvers such as highway merge [12], lane change [13], and intersections [14]. Note that Definition 1 uses constant intent bounds, but our analysis can be adapted to cases where these bounds are time-varying. Also notice that Definition 1 can be naturally extended to describe a vehicle's lateral motion intent using a model and the bounds on the corresponding vehicle states and inputs. These are left as future work.

The next subsection shows how such intent information may be encoded into wireless messages using commercially available V2X communication devices on real vehicles.

B. Implementing Intent Messages

The Definition 1 of intent is implementable for vehicles of different automation levels. To send the intent of a connected automated vehicle, the intended velocity and acceleration bounds may be extracted from its high level motion planner, which prescribes general future behaviors for the vehicle. For a connected human-driven vehicle, on the other hand, such intent bounds may be extracted in a data-driven way from the human driver's historical behaviors when involved in similar scenarios.

To create intent messages, we utilize WAVE Short Message Protocol (WSMP) [15] on commercially available V2X onboard units (OBUs) as shown in Fig. 2(a). Here, WSMP is a network layer messaging protocol allowing the transmission of messages with customized content and packet sending

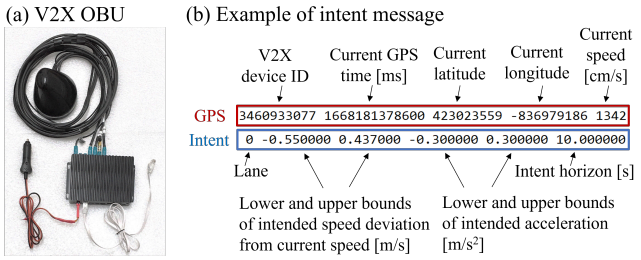

Fig. 2. Creating intent messages. (a) V2X on-board unit. (b) an example of an intent message implemented using V2X protocol WSMP.

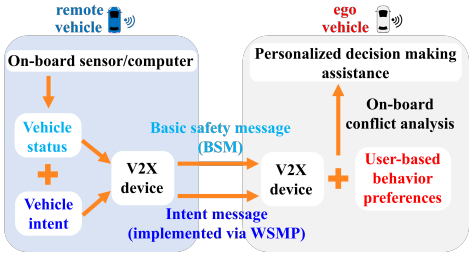

Fig. 3. Schematic diagram of the on-board decision assistance system using status and intent messages based on conflict analysis.

rate. We implement the WSMP-based message transmission in C language using the application programming interface (API) provided by the OBU manufacturer, where we utilized appropriate data structures to store and transmit the parameters representing intent information. Our recent work [16] provides more details of this communication implementation.

Fig. 2(b) shows an example of intent message packet transmitted in our experiment from the remote vehicle traveling with cruise control. This intent message contains the vehicle's current GPS information and motion intent as indicated. Note that the vehicle's intended speed bounds can be constructed by adding the intended speed deviation bounds to its current speed. The values of these bounds were determined based on real data collected from a vehicle running with cruise control, accounting for speed and acceleration errors. Due to the data-compact representation of vehicle intent, our intent message is lightweight (with a size of 51 bytes which may be further reduced using less digits). This contributes to less packet drops and efficient use of communication resources.

In the next section, we build theory for utilizing intent messages to prevent conflicts in cooperative maneuvers.

III. Conflict Analysis

In [12] we proposed a framework of conflict analysis and used it to aid an automated vehicle's decision-making in conflict resolution. In this section, we extend conflict analysis to provide personalized decision-making assistance to a human-driven ego vehicle based on the status and intent information received from the remote vehicle.

We consider that the driver of the ego vehicle has a behavior preference when performing the merge maneuver. Such behavior preference may be represented by restricted ranges of velocity and acceleration during the maneuver. That is, to merge onto the main road, the human driver would drive the ego vehicle such that the following condition is satisfied $\forall t \geq 0$ until exiting the conflict zone:

$$v_0(t) \in [\underline{v}_0(t), \overline{v}_0(t)], \quad u_0(t) \in [\underline{a}_0(t), \overline{a}_0(t)], \tag{5}$$

where the bounds $\underline{v}_0$, $\overline{v}_0$, $\underline{a}_0$, and $\overline{a}_0$ are functions of time t satisfying $\forall t \geq 0$, $v_{\min,0} \leq \underline{v}_0(t) \leq \overline{v}_0(t) \leq v_{\max,0}$ and $a_{\min,0} \leq \underline{a}_0(t) \leq \overline{a}_0(t) \leq a_{\max,0}$; see Fig. 5(a)-(b) for an example of these bounds in merge scenario. Such preference may be extracted in a data-driven manner from the historical data when a specific driver was performing similar maneuvers. Note that the behavior preference bounds in (5) implicitly represent a human driver's behavior uncertainty in performing a given maneuver. Such human uncertainty must be considered in predicting conflicts.

As shown in the diagram in Fig. 3, we aim to build conflict analysis to provide a personalized decision-making assistance to the ego vehicle given its user-based behavior preference. We are interested in whether the human-driven ego vehicle 0 can merge ahead of the remote vehicle 1 without a conflict, while considering the behavior uncertainties of both vehicles. Such no-conflict merge ahead is summarized by the following statement: *independent of the motion of remote vehicle* 1, *the ego vehicle* 0 *is able to merge ahead without a conflict under its human driver's behavior preference*. A conflict-free merge ahead can be formally described by the proposition

$$P := \{\exists t, r_1(t) = 0 \wedge r_0(t) < -s\}, \tag{6}$$

where $\wedge$ is the logical conjunction "and". Then the aforementioned statement corresponds to a subset of the state space Ω of the system (1):

$$\mathcal{P}_{\mathrm{g}} := \{\mathbf{x} \in \Omega | \forall u_1(t), \forall u_0(t), P\}, \tag{7}$$

where the subscript "g" is used following the convention of using green color to visualize a no-conflict set; see also [12].

Once the ego vehicle receives a status message packet from the remote vehicle, we need to check if the current system state $\mathbf{x}$ is in the set $\mathcal{P}_{\mathrm{g}}$, based on the currently available intent information encoded in the latest received intent packet. Note that in practice intent packets may be transmitted at a different rate than the status packets, and the two types of messages may not come in a synchronized manner. If $\mathbf{x} \in \mathcal{P}_{\mathrm{g}}$, a conflict free merge ahead is guaranteed and thus, the ego vehicle's driver can confidently merge ahead. Otherwise, the ego vehicle's driver should yield to the remote vehicle to prevent a potential conflict due to the behavior uncertainties of the remote vehicle and the ego vehicle's human driver. In this case, we issue a warning to the ego vehicle's driver as a decision assistance according to the rule

$$\text{decision} = \begin{cases} \text{merge ahead (no warning)}, & \text{if } \mathbf{x}(t_k) \in \mathcal{P}_{\mathrm{g}}, \\ \text{yield (warning)}, & \text{otherwise}, \end{cases} \tag{8}$$

where t_k, $k = 0, 1, \ldots$ represent the time moments when status information packets are received by the ego vehicle.

At any t_k, let $\tilde{t}_k \leq t_k$ be the latest time when the ego vehicle received an intent packet from the remote vehicle;

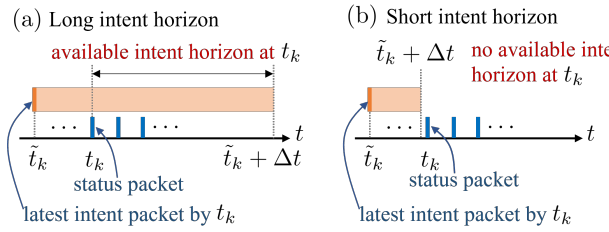

Fig. 4. Schematic visualization of the timing of receiving V2X message packets. (a) An intent packet with long horizon. (b) An intent packet with short horizon and low sending frequency.

see Fig. 4(a) for a schematic visualization of the message timing. Here, we assume that the status and intent message packets, once generated on the remote vehicle, are delivered to the ego vehicle with ignorable transmission time delay. We present the following Theorem, which provides a criterion for the ego vehicle to examine if $\mathbf{x}(t_k) \in \mathcal{P}_{\mathrm{g}}$, using the latest available intent information.

Theorem 1: Given the dynamics (1)-(2), the current system state $\mathbf{x}(t_k)$, the ego vehicle driver's behavior preference (5), and the remote vehicle's intent information $v_1(t) \in [\underline{v}_1, \overline{v}_1]$, $u_1(t) \in [\underline{a}_1, \overline{a}_1]$, $t \in [\tilde{t}_k, \tilde{t}_k + \Delta t]$, we have

$$\mathbf{x}(t_k) \in \mathcal{P}_{\mathrm{g}} \iff T^{\mathrm{est}}_{\mathrm{exit},0} < T^{\mathrm{est}}_{\mathrm{reach},1}, \tag{9}$$

where $T^{\mathrm{est}}_{\mathrm{exit},0}$ is the time t such that $r_0(t) = -s$ under

$$u_0(t) \equiv \underline{a}_0(t), \quad t \geq t_k, \tag{10}$$

and $T^{\mathrm{est}}_{\mathrm{reach},1}$ is the time t such that $r_1(t) = 0$ under

$$u_1(t) = \begin{cases} \overline{a}_1, & \text{if } t \in [t_k, \tilde{t}_k + \Delta t), \\ a_{\max,1}, & \text{otherwise.} \end{cases} \tag{11}$$

Proof: See Appendix I. ∎

As illustrated in Fig. 1(b), $T^{\mathrm{est}}_{\mathrm{exit},0}$ represents the estimated time of the ego vehicle exiting the conflict zone under worst-case behavior (input lower bound) considering human behavior uncertainty (5). Also, $T^{\mathrm{est}}_{\mathrm{reach},1}$ represents the estimated time when the remote vehicle reaches the conflict zone under its worst future behavior (input upper bound) given by the available intent information; see Fig. 4(a). We emphasize that intent information leads to less uncertainty in the ego vehicle's estimation on the evolution of its future environment, resulting in more efficient decision-making. Note that if intent packet covers only a short horizon while being sent at a low frequency such that $t_k \geq \tilde{t}_k + \Delta t$ holds in (11); see Fig. 4(b), then the latest intent information is already expired at t_k, which shall be no longer used in the calculation. In this case, (11) converts to $u_1(t) \equiv a_{\max,1}$ for $t \geq t_k$. This indicates that intent messages shall be transmitted with an appropriate sending rate and horizon to maintain a good performance. The effects of these parameters will be evaluated in the next section using experimental data.

In summary, Theorem 1 provides an efficient algorithm to check if conflict-free merge ahead is guaranteed (i.e., $\mathbf{x}(t_k) \in \mathcal{P}_{\mathrm{g}}$), using two time parameters $T^{\mathrm{est}}_{\mathrm{exit},0}$ and $T^{\mathrm{est}}_{\mathrm{reach},1}$, which can be numerically calculated. This enables personalized decision-making assistance for the ego vehicle's nonconflicting maneuvers based on status and intent information. In the next section, this algorithm is implemented on real connected vehicles to experimentally evaluate the benefits of intent sharing.

IV. Experiments

We performed experiments at the Mcity test track at the University of Michigan using real vehicles equipped with V2X OBUs. The experimental setup is shown in Fig. 1(a), where the blue remote vehicle travels along the main road, while the white ego vehicle attempts to merge onto the main road within a merge zone of length 50 [m]. The conflict zone was set to be 20 [m] long. Note that we set up the merge zone not corresponding to the Mcity on-ramp to enable us to use a longer straight section of the main road. Both vehicles are human-driven, and for safety reason, the remote vehicle used the second to the rightmost lane on the main road. This allows us to study conflicts without endangering the participants. The speed of the human-driven remote vehicle was regulated by cruise control (set to 30 [mi/hr] ≈ 13.4 [m/s]); see Fig. 5(a)-(b) for remote vehicle's data in one of the experiments. The status (position r_1 and velocity v_1) of the remote vehicle is transmitted via BSMs every 0.1 [s], while the cruise control intent was encoded in intent messages as described in Section II-B and transmitted every 1 [s]. An example of such intent is visualized in Fig. 5(a)-(b) by the light blue area, which highlights the remote vehicle's intent shared at the initial time with a horizon of 10 [s]. The corresponding intent parameters were the same as in the intent message example shown in Fig. 2(b).

In the merge experiment, the initial time was defined as the time when the remote vehicle was 150 [m] away from the conflict zone. The ego vehicle started from standstill with its initial position at the beginning of the merge zone (30 [m] away from the conflict zone). We emphasize that such setup models a merge scenario commonly seen in the US expressways. We extracted the behavior preference of the ego vehicle's driver by collecting data of the driver's normal merge maneuver under the same road setup. Fig. 5(a)-(b) show the extracted upper and lower bounds of the driver's speed and acceleration preference, where the gray region between the bounds represents the human driver's behavior uncertainty. A computer was used inside the ego vehicle to record the received BSMs and intent messages, and to implement the conflict analysis algorithm in Theorem 1 via MATLAB for on-board decision assistance real time.

Two types of experiments were performed: **(i)** as the remote vehicle approached, the ego vehicle was stationary at its initial position while conducting conflict analysis based on the received messages, and on-board warning was issued under decision rule (8); **(ii)** as the remote vehicle approached, the ego vehicle's human driver started to merge onto the main road with different start times before or after the warning was issued. Note that the warning was generated as an audible sound from the computer running conflict analysis, with a warning message displayed on the screen. Experiments of **type (i)** allowed us to test the utility of intent sharing in conflict resolution, and to evaluate the benefits of intent

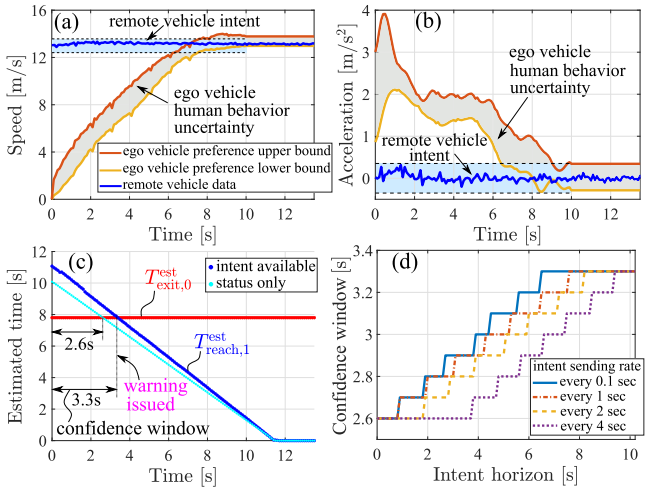

Fig. 5. Evaluating the benefits of intent messages. (a)-(b) remote vehicle's profiles and ego vehicle's behavior bounds in an experiment where ego vehicle stayed standstill in front of merge zone while performing on-board conflict analysis. (c) Evolution of estimated times $T^{\text{est}}_{\text{exit},0}$ and $T^{\text{est}}_{\text{reach},1}$ (intent-based and status-based). (d) Confidence window as a function of intent horizon under different intent sending rates.

sharing under different communication conditions. On the other hand, by varying the merge starting time of a real human driver, experiments of **type (ii)** allowed us to validate the on-board decision assistance. The next two subsections give details on these two types of experiments respectively. Note that the results presented below are based on the actual codes that were run during the experiments real time.

A. Evaluating Intent Sharing

The leftmost column of Fig. 1(a) shows camera views from the ego vehicle's rear mirror during an experiment of **type (i)**, with the corresponding decision assistance highlighted. When the remote vehicle was far away, no conflict was predicted and thus, no warning was issued. As the remote vehicle approached, our framework predicted a conflict is possible between the ego and remote vehicle, and a warning was issued. The warning persisted until the remote vehicle passed the ego vehicle. The conflict analysis of this experiment is visualized in Fig. 5(c), where the estimated times $T^{\text{est}}_{\text{exit},0}$ and $T^{\text{est}}_{\text{reach},1}$ were calculated at each BSM receiving time under the available intent information. With cruise control intent, the warning was issued after 3.3 [s] when $T^{\text{est}}_{\text{exit},0} \geq T^{\text{est}}_{\text{reach},1}$ held; cf. Theorem 1 and (8). Before the warning is issued, the ego vehicle's human driver may confidently pursue the merge ahead opportunity. We refer to such time segment the confidence window.

On the other hand, if intent messages had not been shared, then the values of $T^{\text{est}}_{\text{reach},1}$ become smaller under status information only; see the cyan curve in Fig. 5(c). In this case, the warning would be issued earlier, yielding a shorter confidence window of 2.6 [s]. We emphasize that such unnecessarily early warning can cause the human driver to miss the opportunity of a conflict-free merge ahead, resulting in a significantly delayed merge. Thus, confidence window can be used as a metric to quantify the benefits of intent sharing. With the cruise control intent shared in this experiment, the confidence window achieved a 27% increase. Therefore, intent sharing contributes to a more efficient decision, better time efficiency, and improved traffic throughput.

To evaluate the effects of different intent sending conditions on the gained benefits, we performed post-experiment simulations using the collected data. Fig. 5(d) quantifies the confidence window as a function of intent horizon under different intent sending rates. As the horizon increases, confidence window increases until saturating, and higher sending rate contributes to larger window size. The discrete jumps in these plots are due to the fact that decision for the ego vehicle is evaluated at the discrete times when BSMs were received (every 0.1 [s]).

B. Validating Intent-based On-board Decision Assistance

Now we focus on experiments of **type (ii)**, where the on-board conflict analysis was conducted similarly as described in the previous subsection, but the ego vehicle's driver initiated the merge maneuver with selected start times before or after the warning was issued. Fig. 6(a)-(c) illustrate a sequence of the aerial views and the corresponding on-board conflict analysis during one such experiment, where the human driver started to merge when the warning was already issued; see Fig. 6(b). Here, $T^{\text{est}}_{\text{exit},0}$ decreased at around 5.4 [s] as the ego vehicle started to move (with an actual behavior better than the worst-case input used in prediction). As shown by Fig. 6(c), violating the warning resulted in a conflict with the remote vehicle. Note that the generated warning was personalized based on the behavior preference of the ego vehicle's driver.

Similar experiments were conducted for different merge starting times. We summarize the results in Fig. 7, where each data point represents an experiment, showing the merge initiation time of the ego vehicle and the corresponding position of the remote vehicle. The data points are colored according to the merge results as indicated. We observed that initiating the merge before the warning always led to a conflict-free merge ahead; see blue points and the average confidence windows overlapped in Fig. 7. When merging slightly after the warning, the ego vehicle was still able to perform a conflict-free merge ahead; see yellow points. This conservatism of the warning system was because our on-board conflict analysis used the ego driver's worst-case behavior (under the known preference) to account for human behavior uncertainty, while the human's actual behavior was often better than this. Notice that for these cases, our on-board warning was able to disappear automatically during the maneuver based on the calculation of $T^{\text{est}}_{\text{exit},0}$ and $T^{\text{est}}_{\text{reach},1}$ using the updated status and intent information. This demonstrated the real-time decision assistance capability. On the other hand, the necessity of the aforementioned conservatism in decision assistance was also justified by a segment mixed with yellow and red points, where conflicts could happen depending on the driver's actual behaviors. As the remote vehicle has got closer, initiating a conflict-free merge ahead was no longer possible amid the warning, but the ego vehicle's driver was able to realize a conflict-free merge behind; see green points.

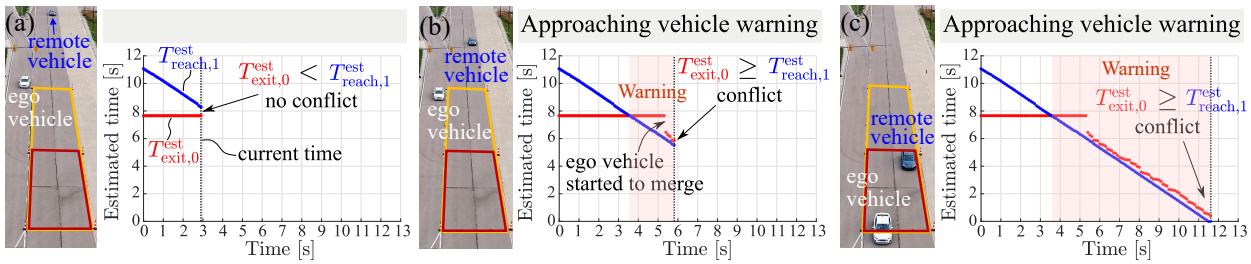

Fig. 6. An experiment where the ego vehicle started to merge after the warning was issued and ended up in a conflict with the remote vehicle. For each panel (a)-(c), left: bird's eye view of the experiment; right: ego vehicle's on-board conflict analysis and warning.

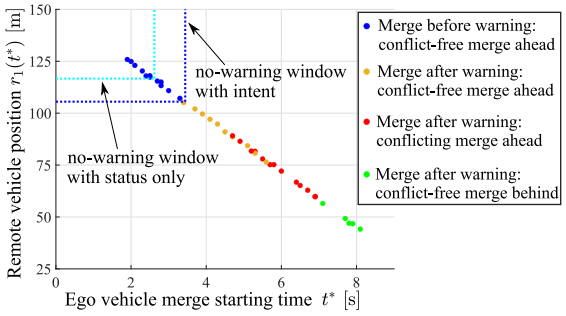

Fig. 7. Experimental validation of the intent-based on-board decision assistance system, where the remote vehicle traveled with cruise control and the ego vehicle was driven by a human driver. Ego vehicle's driver started to merge with different timings, before and after the warning was issued, which led to the indicated results.

In summary, these results show that the intent-based warning system was able to provide personalized decision assistance to enhance the safety of the human-driven merging vehicle, while violating such warning could lead to conflicts.

V. Conclusion

In this paper we implemented intent sharing communication using real vehicles, where future motion information of a vehicle was encoded into intent messages and transmitted via commercially available V2X devices. We experimentally demonstrated that compared to receiving status information only, additional intent information can significantly benefit a vehicle's decision and time efficiency by reducing uncertainty in predicting future conflicts with other vehicles in cooperative maneuvers. Using conflict analysis, we quantified these merits and evaluated the effects of intent transmission conditions (sending rate and horizon) on these benefits. Moreover, we validated an on-board decision assistance system that helps a human driver make a personalized safe decision in merge scenarios using the received status and intent information. Our future work includes considering more detailed intent information and extending the experimental work to automated vehicles.

Appendix I
Proof of Theorem 1

($\Rightarrow$). If $\mathbf{x}(t_k) \in \mathcal{P}_{\text{g}}$, then for the inputs u_0 and u_1 in (10) and (11), we have $\exists t, r_1(t) = 0 \wedge r_0(t) < -s$. Such t must be unique since $r_1(t)$ is monotonic along t, implying $t = T^{\text{est}}_{\text{reach},1}$. Thus, $T^{\text{est}}_{\text{exit},0} < T^{\text{est}}_{\text{reach},1}$ holds obviously.

($\Leftarrow$). If $T^{\text{est}}_{\text{exit},0} < T^{\text{est}}_{\text{reach},1}$, then for the inputs u_0 and u_1 in (10) and (11), $\exists t = T^{\text{est}}_{\text{reach},1}, r_1(t) = 0 \wedge r_0(t) < -s$. For arbitrary u_0 and u_1 other than (10) and (11), let $\tilde{T}^{\text{est}}_{\text{exit},0}$ and $\tilde{T}^{\text{est}}_{\text{reach},1}$ be the times such that $r_0(t) = -s$ and $r_1(t) = 0$. We have $\tilde{T}^{\text{est}}_{\text{exit},0} < T^{\text{est}}_{\text{exit},0} < T^{\text{est}}_{\text{reach},1} < \tilde{T}^{\text{est}}_{\text{reach},1}$, which yields $\exists t = \tilde{T}^{\text{est}}_{\text{reach},1}, r_1(t) = 0 \wedge r_0(t) < -s$. Thus, $\mathbf{x}(t_k) \in \mathcal{P}_{\text{g}}$.

References

[1] L. Hobert, A. Festag, I. Llatser, L. Altomare, F. Visintainer, and A. Kovacs, "Enhancements of V2X communication in support of cooperative autonomous driving," *IEEE Communications Magazine*, vol. 53, no. 12, pp. 64–70, 2015.

[2] I. Llatser, T. Michalke, M. Dolgov, F. Wildschütte, and H. Fuchs, "Cooperative automated driving use cases for 5G V2X communication," in *2nd IEEE 5G World Forum (5GWF)*, 2019, pp. 120–125.

[3] B. Lehmann, H.-J. Günther, and L. Wolf, "A generic approach towards maneuver coordination for automated vehicles," in *2018 21st International Conference on Intelligent Transportation Systems (ITSC)*. IEEE, 2018, pp. 3333–3339.

[4] C. Liu, C.-W. Lin, S. Shiraishi, and M. Tomizuka, "Distributed conflict resolution for connected autonomous vehicles," *IEEE Transactions on Intelligent Vehicles*, vol. 3, no. 1, pp. 18–29, 2020.

[5] J. Rios-Torres and A. A. Malikopoulos, "A survey on the coordination of connected and automated vehicles at intersections and merging at highway on-ramps," *IEEE Transactions on Intelligent Transportation Systems*, vol. 18, no. 5, pp. 1066–1077, 2016.

[6] SAE J3016, "Taxonomy and Definitions for Terms Related to Driving Automation Systems for On-Road Motor Vehicles," SAE International, Tech. Rep., 2021.

[7] SAE J3216, "Taxonomy and Definitions for Terms Related to Cooperative Driving Automation for On-Road Motor Vehicles," SAE International, Tech. Rep., 2020.

[8] SAE J2735, "Dedicated Short Range Communications (DSRC) Message Set Dictionary Set," SAE International, Tech. Rep., 2016.

[9] SAE J3186, "Application Protocol and Requirements for Maneuver Sharing and Coordinating Service," SAE International, Tech. Rep., work in progress. Available: https://www.sae.org/standards/content/j3186/.

[10] *Intelligent Transport Systems (ITS); Vehicular Communications; Informative report for the Maneuver Coordination Service*, ETSI TR 103 578 Std., draft 0.0.7, Feb. 2022.

[11] A. Correa, R. Alms, J. Gozalvez, M. Sepulcre, M. Rondinone, R. Blokpoel, L. Lücken, and G. Thandavarayan, "Infrastructure support for cooperative maneuvers in connected and automated driving," in *IEEE Intelligent Vehicles Symposium (IV)*. IEEE, 2019, pp. 20–25.

[12] H. M. Wang, S. S. Avedisov, T. G. Molnár, A. H. Sakr, O. Altintas, and G. Orosz, "Conflict analysis for cooperative maneuvering with status and intent sharing via V2X communication," *IEEE Transactions on Intelligent Vehicles*, vol. 8, no. 2, pp. 1105–1118, 2023.

[13] H. M. Wang, S. S. Avedisov, O. Altintas, and G. Orosz, "Multi-vehicle conflict management with status and intent sharing under time delays," *IEEE Transactions on Intelligent Vehicles*, vol. 8, no. 2, pp. 1624–1637, 2023.

[14] S. S. Avedisov, A. H. Sakr, T. Higuchi, and O. Altintas, "Cooperative perception based on intent-sharing messages," in *2023 IEEE Vehicular Networking Conference*, to be published.

[15] *IEEE Standard for Wireless Access in Vehicular Environments (WAVE)–Networking Services*, IEEE Std., 1609.3-2020, Dec. 2020.

[16] H. M. Wang, S. S. Avedisov, O. Altintas, and G. Orosz, "Evaluating intent sharing communication using real connected vehicles," in *2023 IEEE Vehicular Networking Conference*, to be published.